

## ARTICLES

Molecular Dynamics Simulation Study of 18-Crown-6 in Aqueous Solution. 2. Free Energy Profile for the Association  $18C6 \cdot \cdot K^+$  in WaterThomas Kowall<sup>†</sup> and Alfons Geiger\**Physikalische Chemie, Fachbereich Chemie der Universität Dortmund, D-44221 Dortmund, Germany*Received: March 23, 1994; In Final Form: July 27, 1994<sup>®</sup>

The free energy profile for the association of  $18C6 \cdot \cdot K^+$  in water is investigated employing the umbrella sampling technique. By a specific bias potential the encounter geometry of crown and ion is restricted to a mutual approach along the crown's symmetry axis. The most striking feature in the computed  $W(r)$  is a solvent-bridged pair  $18C6 \cdot \cdot H_2O \cdot \cdot K^+$  as a distinct local free energy minimum. The bridging water molecule—strongly hydrogen bonded to 18C6 and already preformed without an ion present—is capable of simultaneously and efficiently docking with the  $K^+$  ion. The presence of a free energy activation barrier is in qualitative accord with experimental findings. Discrepancies with former theoretical results lacking such a barrier are discussed.

## 1. Introduction

To study the stability of an associate  $A \cdot \cdot B$  in a solvent, a simple molecular mechanics approach involving potential energies *in vacuo* is in general no longer adequate. The property needed is the free energy difference between the separately solvated solutes A and B and the solvated complex  $A \cdot \cdot B$ . One of the advantages of molecular dynamics simulations is the capability of evaluating free energy differences between two adjacent states of a system or even the entire free energy profile along any chosen reaction path in a solvent.

The free energy profile  $W_{AB}(r)$  along the distance coordinate  $r$  of two solutes A and B in a solvent (averaged over all other geometric and conformational degrees of freedom) equals the reversible work to move A and B from an infinite separation to a distance  $r$ . In comparison to the potential energy  $U_{AB}(r)$  *in vacuo* ("direct interaction")  $W_{AB}(r)$  provides insights into the solvent's impact on the interaction of A and B. For charged or polar particles this is a shielding proportional to the (local) dielectricity constant of the model solvent. Beyond that in numerous cases an oscillating behavior has been observed, where a solvent-bridged state " $A \cdot \cdot \text{solvent} \cdot \cdot B$ " constitutes a local free energy minimum of its own and is separated from the contact pair by a free energy barrier (e.g. argon/argon,<sup>1</sup>  $Na^+/Cl^-$ ,<sup>2</sup>  $Cl^-/Cl^-$ ,<sup>3</sup> benzene/benzene,<sup>4</sup>  $AcO^-/C(NH_2)_3^{+5}$ ).

A conventional MD simulation generates a distribution of configurations weighted according to their Boltzmann factor. In this way "mechanical" properties such as energy or pressure can be evaluated by straightforward averaging without explicit knowledge of the partition function. This is in general not valid for the partition function itself or related entropic properties such as free energies. For the calculation of the profile of relative free energies  $W_{AB}(r)$  on the basis of a MC or MD simulation various methods are at one's disposal (e.g. perturbation method,<sup>6</sup> thermodynamic integration,<sup>7</sup> and umbrella sampling<sup>1,8</sup> that have been applied in the literature to several pairs of atomic and molecular species.

Usually, the results obtained on identical systems by different potential models and free energy techniques agree qualitatively, but exhibit greater deviations in a quantitative regard (cf. refs 9 and 10 for  $18C6 \cdot \cdot K^+$  or the compilation of literature results for the pair  $Na^+/Cl^-$  in water.<sup>11</sup>). For the quite fundamental system  $Cl^-/Cl^-$  in water even the qualitative appearance of  $W_{AB}(r)$  has been under debate.<sup>3,12</sup>

Recently, two independent studies treating the free energy profile  $W(r)$  for the association of the crown ether 18C6 and  $K^+$  in water were reported. van Eerden et al.<sup>9</sup> made use of thermodynamic integration in a united atom approach, whereas Dang and Kollman<sup>10</sup> applied the perturbation method with an "all-atom force field". The profiles  $W(r)$  obtained in refs 9 and 10 proved to be in accord in a rough, qualitative manner, but differed quantitatively to a substantial extent. In ref 10 a very good reproduction of the experimental free energy of binding is achieved. As already mentioned in ref 9, a considerable free energy barrier for the complexation/decomplexation process was derived experimentally,<sup>13</sup> while in refs 9 and 10 such a barrier is lacking except for a plateau region.

After a detailed study of the structure and dynamics of the hydration shell of a single crown ether molecule and of the complex  $18C6 \cdot \cdot K^+$  (ref 14, henceforth referred to as part 1), we now study the potential of mean force  $W(r)$  and test the results of refs 9 and 10 by another technique (umbrella sampling<sup>1</sup>) and for another potential model. Special interest is directed toward possible, yet undetected, barriers. Due to obvious sampling and normalization difficulties, a convenient bias potential has to be introduced that imposes a well-defined reaction path by restricting the relative orientation of crown and ion to a certain range without causing uncontrollable artifacts.

## 2. Methods

**2.1. Umbrella Sampling.** The radial pair distribution function  $g_{AB}(r)$  between two solutes A and B determines the free energy profile  $W_{AB}(r)$  except for an additive constant:<sup>15</sup>

$$W_{AB}(r) = -k_B T \ln g_{AB}(r) + C$$

The function  $W_{AB}(r)$ —for molecular species A or B averaged

<sup>†</sup> Present address: Institut de chimie minérale et analytique, Université de Lausanne, CH-1005 Lausanne, Switzerland.

<sup>®</sup> Abstract published in *Advance ACS Abstracts*, March 1, 1995.

over all relative orientations of A and B and all accessible conformers—determines the free energy of complexation  $\Delta G_b$ . For 18C6/K<sup>+</sup> in water  $\Delta G_b$  amounts to  $-12$  kJ/mol.<sup>16</sup>  $\Delta G_b$  on the order of several  $k_B T$  implies that in an equilibrated MD simulation nearly exclusively associated configurations will show up. One has to take into account that in view of typical complexation/decomplexation times of  $10^{-6}$  s for {18C6/K<sup>+</sup>}<sub>aq</sub><sup>17</sup> no equilibrated distance distribution 18C6••K<sup>+</sup> is achievable by MD simulations of a few hundred picoseconds. For the above relation to be applicable, however,  $g_{AB}(r)$  must be known over a wide separation range with equal accuracy. The umbrella sampling technique, used in this work to calculate  $g_{AB}(r)$ , eliminates the need for exceedingly long MD runs.

By an additional bias potential  $U_B(\vec{r}_{AB})$ , generally harmonic, both solutes A and B are confined to a certain distance range, and a biased distribution function  $g_{AB}^*(r)$  is obtained. From quantities computed for the biased system ( $U + U_B$ ) one is able to calculate back the desired unbiased distribution function:<sup>1</sup>

$$g_{AB}(r) = g_{AB}^*(r) \frac{e^{+U_B(r)/RT}}{\langle e^{+U_B(r)/RT} \rangle_{U+U_B}}$$

In practice, in several consecutive simulations harmonic bias potential are shifted systematically along the total separation range, and the results are assembled afterwards. For a given system convenient bias potentials have to be found empirically by pretrial runs in order to minimize the number of overlapping distance windows. In a “matching procedure”<sup>1</sup> subsequent to the simulation, for each window a scaling factor is determined in such a way that the distribution functions for the different sections coincide in their overlapping parts, and a steady  $g(r)$  results.

Umbrella sampling has in common with the alternative techniques of thermodynamic integration and the perturbation method that they merely yield the static function  $W(r)$ . Dynamical information, e.g. how often a free energy barrier (e.g. between the contact pair and solvent-bridged pair) is crossed, is lacking.<sup>1</sup>

**2.2. Restriction of the Relative Orientation of 18C6 and K<sup>+</sup>.** In the classical version of umbrella sampling two atomic particles A and B in a solvent are confined to a certain distance range around  $|\vec{r}_{AB}|$ ; apart from that, A and B are free to move around each other in spherical shells.<sup>1</sup> Within each window the sampled volume increases  $\propto r^2$ , which is corrected for, when normalizing  $g(r)$ . In the majority of previously reported umbrella sampling—MD studies the accessible volume has been reduced further by additionally restricting the direction of the distance vector, typically along the  $z$ -axis (e.g. refs 2, 3). In practice, particle A is completely fixed by imposing a large mass, and a stiff harmonic potential  $U_{xy}$  for the  $xy$ -displacement is introduced, which solely acts on particle B. The underlying reason for this procedure is that otherwise for fairly short simulation runs per window the actually explored volume would not increase ideally  $\propto r^2$  and the necessary normalization of  $g(r)$  would remain obscure. Moreover, as an economical advantage such a procedure allows using a rectangular tetragonal MD box that is to be elongated only in the  $z$ -direction.

For the *molecular* system 18C6••K<sup>+</sup>, restricting the distance vector's direction is important for another reason, too. In this case the free energy profile also depends on the direction along which the ion approaches; explicitly, assuming an approximate cylindrical symmetry, it depends on the elevation angle  $\theta$  with respect to the crown's plane. To get  $W(r)$ , averaging of  $W(r, \theta)$  has to be performed over all orientations  $\theta$ . However such an averaging cannot be accomplished in a few hundred picoseconds

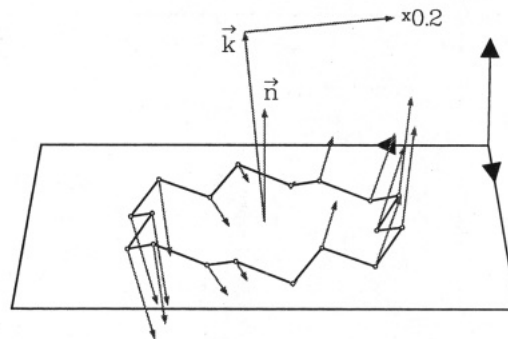


**Figure 1.** Example of the back-driving forces acting on K<sup>+</sup> and the ether atoms, when the ion at  $\vec{k}$  deviates from the direction of the crown's symmetry axis  $\vec{n}$ .

per window. For polyatomic molecules Pettitt and Karplus<sup>18</sup> suggest, therefore, that “a set of angular constraining potentials chosen to cover the mutual angular degrees of freedom between the solutes would have to be employed at every separation distance”. In this spirit we sample a well-defined section of the full free energy surface  $W(r, \theta)$  by applying an extended procedure that restricts the relative orientation of crown and ion during their approach preferably along the crown's symmetry axis. Beyond that the pair {18C6••K<sup>+</sup>} is free to translate and rotate as a whole. For this purpose the radial bias potential  $V_{US}(r) = \frac{1}{2}K_{US}(r - r_0)^2$  is supplemented by an additional “deformation” potential  $V_\theta(\theta) = \frac{1}{2}K_\theta(\theta - \theta_0)^2$  for the angle  $\theta$  between the crown's symmetry axis  $\vec{n}$  and the vector  $\vec{k}$  connecting the ion and the crown's center-of-mass.

The force  $\vec{F}_{\theta,i}$  acting on atom  $i$  due to the potential  $V_\theta$  is

$$\vec{F}_{\theta,i} = -K_\theta(\theta - \theta_0) \frac{\delta\theta}{\delta\vec{r}_i}$$

For K<sup>+</sup> the required gradient  $\delta\theta/\delta\vec{r}_i$  is evaluated, analytically by analogy with the deformation term in flexible molecules. For the crown atoms  $\delta\theta/\delta\vec{r}_i$  is calculated numerically from the displacement  $\Delta\vec{r}_i$  when (imaginarily) rotating the crown molecule around the axis  $\vec{n} \times \vec{k}$  by a differential angle  $\Delta\theta$ . In this way the resulting torque acting on {18C6••K<sup>+</sup>}—along the direction  $\vec{n} \times \vec{k}$  with respect to the common center-of-mass—cancels. The total force on the center-of-mass is compensated by an additional counteracting force. Figure 1 illustrates the acting forces.

By contrast to MD simulations, in MC studies the relative orientation of two molecules can be handled more easily by displacing the molecules only along their connecting line. Therefore, MC studies have been used preferably for  $W(r)$  calculations involving polyatomic molecules (e.g. AcO<sup>-</sup>/C(NH<sub>2</sub>)<sub>3</sub><sup>+</sup>,<sup>5</sup> amide/amide,<sup>19</sup> (CH<sub>3</sub>)<sub>3</sub>C<sup>+</sup>/Cl<sup>-</sup>,<sup>20</sup> benzene/benzene,<sup>4</sup> C(NH<sub>2</sub>)<sub>3</sub><sup>+</sup>/C(NH<sub>2</sub>)<sub>3</sub><sup>+</sup>). Two MD studies by Dang and Kollman applying the perturbation method constitute an exception. In ref 22 two nucleobases and in ref 10 the crown ether 18C6 and a K<sup>+</sup> ion have been *completely* fixed in their relative orientation, although without stating by which means this has been accomplished.

**2.3. Simulation Parameters.** A tetragonal MD box with an elongated  $z$ -axis bears no advantage, since the associate 18C6••K<sup>+</sup> is allowed to rotate freely. As in the previous simulations, a truncated octahedron was used. For the water—water interaction a cutoff of 9.0 Å, for both crown—water and ion—water a cutoff of 9.5 Å, and for the crown—ion interaction no cutoff was applied. According to these cutoff radii the primary cell was set up sufficiently large for a maximum crown—ion separation of about 7.0 Å (Table 1). During the mutual approach the simulations were started with a configu-

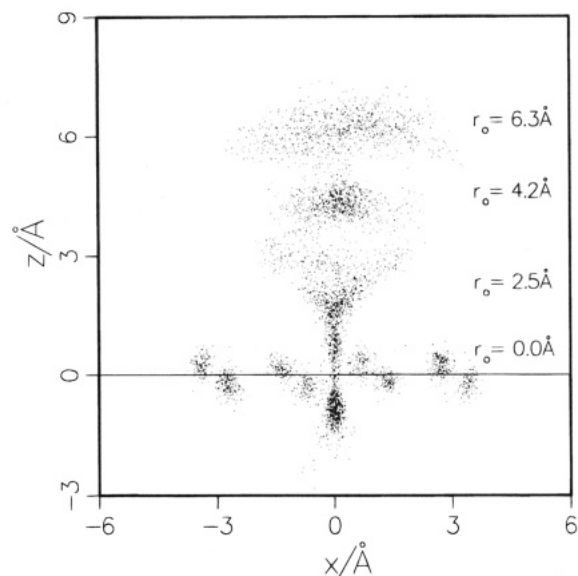


**Figure 2.** "Dot plot" illustrating the ion's residence range for four umbrella-windows (after proper rotation of crown into *xy*-plane).

**TABLE 1: Simulation Parameters**

number of water molecules	618
average size of the trunc octahedron	33.6 Å
time step	2 fs
$\tau_T$	0.1 ps
$\tau_p$	3.0 ps
number of steps per window	65 536
stored configurations per window	4096
$\langle T \rangle / K$	300.4
$\langle p \rangle / \text{bar}$	1.5

ration from a previous run where crown and ion were just separated by the new reference distance. Before storing configurations the crown's translational and rotational momenta were removed, after a few steps the system's total momentum was stopped, and a 16 ps equilibration run was inserted.

The applied constants for the bias potentials are compiled in Table 2. The term  $r_{\text{max}}$  refers to the position of the maximum in the resulting uncorrected distance distribution. For  $r_0 = 0.0$  Å simulation B of part 1 (refer to Table 3 there) was analyzed with only 254 water molecules, but a larger simulation time of 262 ps. For further details of the simulation, in particular the used interaction potentials and the crown ether's conformation, see part 1. Here we just want to summarize that we use one of the standard simulation packages (GROMOS) with a few improvements of the potential parameter set. For example, torsion potentials and partial charges of the crown ether have been taken from quantum mechanical ab initio computations. Moreover, Lennard-Jones parameters for the cation are taken which had been optimized to reproduce the free energy of hydration of  $K^+$  with the SPC water model of GROMOS.

### 3. Results

**3.1. The Free Energy Profile  $W(r)$ .** To visualize the simulated association process, the ion's positions have been accumulated in Figure 2. for four umbrella-windows (superposition of crown molecules and rotation of coordinate system as in Figure 4 of part 1). The volume of the spherical shell segments accessible within a window depends on the separation  $r$ . When calculating the respective sections of  $g^*(r)$  and  $g(r)$ , this is taken into account by a factor  $1/r^2$ . For  $r \rightarrow 0$  this route is no longer practical. Therefore, in the region  $r < 1.5$  Å no longer the ion's distance from the crown's center but the perpendicular distance from the crown's plane is taken as the

**TABLE 2: Constants for Umbrella Sampling–Bias Potentials**

	$r_0, \text{Å}$									
	7.0	6.3	5.6	4.9	4.2	3.5	3.0	2.7	1.5	0.0
$r_{\text{max}}, \text{Å}$	6.8	6.3	5.9	4.7	4.4	4.2	3.6	2.7	1.4	0.9
$K_{\text{US}}, \text{kcal}/(\text{mol Å}^2)$	3.5	3.5	3.5	3.5	3.0	3.0	3.0	7.5	4.5	0.04
$K_\theta, \text{kcal}/(\text{mol rad}^2)$	35.0	30.0	28.0	25.0	20.0	14.0	5.0	5.0	0.0	0.0

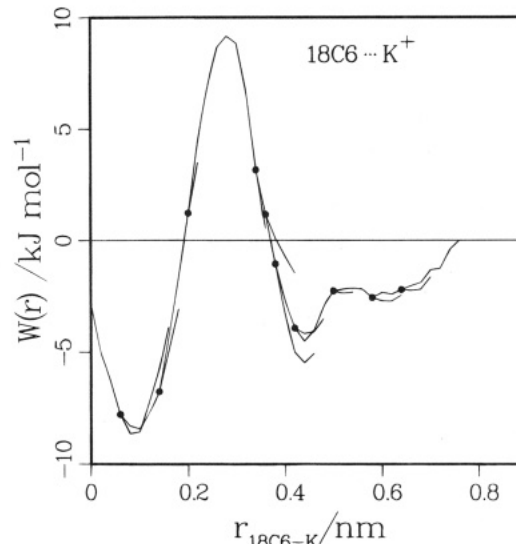


**Figure 3.** Free energy profile  $W(r)$  between 18C6 and  $K^+$  in water.

proper coordinate, and the accessible volume is regarded as independent of the separation. In Figure 3 the resulting  $W(r) = -RT \ln g(r)$  is depicted. The black circles indicate the junctions where the umbrella-windows have been fit together.

In  $W(r)$  the strong shielding due to the solvent is apparent. The most conspicuous feature, however, is the oscillating behavior and the existence of a free energy activation barrier at  $r = 2.8$  Å between a contact and a solvent-bridged state (at  $r = 4.3$  Å and  $r = 0.9$  Å, respectively). A water molecule, situated above the crown's center, which can interact with both crown and ion simultaneously, has already been identified as being present in the binary system 18C6/water (see part 1). This molecule proves to be effective in blocking the host–guest association, even though it can only coordinate two out of three oxygens on each side of the crown at the same time. Figure 4 displays a corresponding snapshot of crown and ion together with 10 nearest water molecules. In the simulation with the umbrella potential around  $r_0 = 2.5$  Å the ion illustratively underwent a transition from the contact to the solvent-bridged state (Figure 5). A hint for even a second by a far smaller barrier at  $r = 5.4$  Å (Figure 3) gives evidence of umbrella sampling's capability of resolving faint details. This feature can be likely ascribed to a transition state between a solvent-bridged and a further solvent-separated pair.

The fact that the ion has to surmount a barrier at  $r = 0.0$  Å when penetrating the crown's plane or, vice versa, that the absolute free energy minimum is situated outside the crown center at  $r = 0.9$  Å conforms with the results in ref 9 and 10. In part 1 an oscillating motion of  $K^+$  through the center of the ring has been observed, which confirms this finding clearly.

In accord with previous observations,<sup>10</sup> this strongly deviates from the potential energy contour of the 18C6/ $K^+$  pair *in vacuo*, which is given in Figure 6. There, a smooth, barrierless energy surface with its minimum in the center of the ether ring is observed.

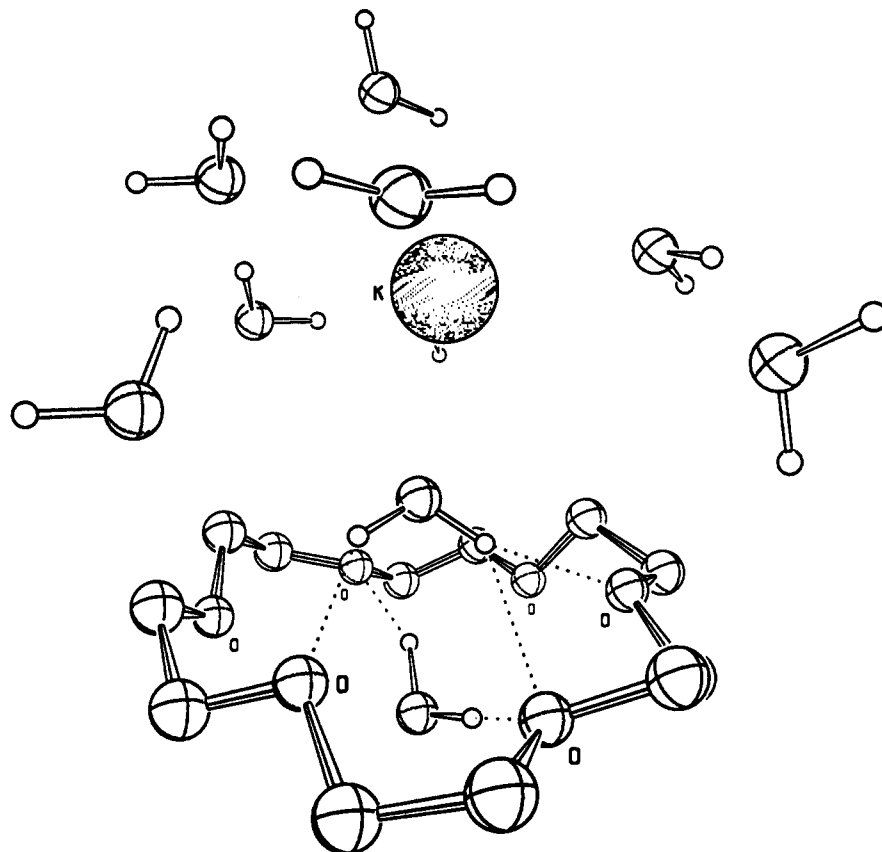


**Figure 4.** Snapshot from the MD simulation for a 18C6··K<sup>+</sup> distance of 4.31 Å, corresponding to the second minimum of  $W(r)$  in Figure 3.

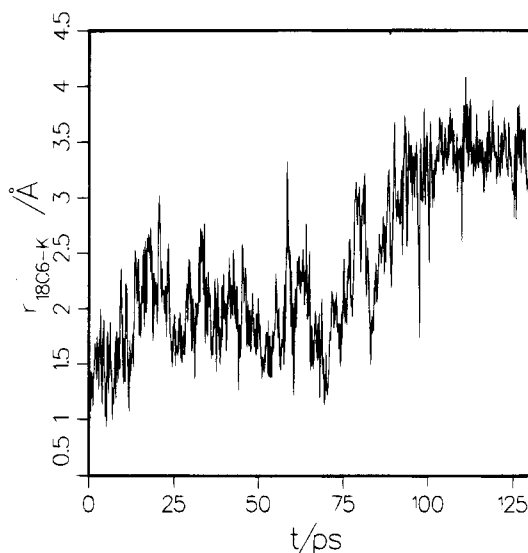


**Figure 5.** Separation ether-cation versus time for the umbrella-window  $r_0 = 2.5$  Å, illustrating a transition from the contact to the solvent-bridged state of K<sup>+</sup>.

**3.2. Short-Time Dynamics of the K<sup>+</sup> Ion.** The change in the short-time dynamics of K<sup>+</sup> when passing from the water cage to the crown cage can be pursued by means of its velocity autocorrelation function (VACF)  $c_{vv}(t)$  and the corresponding frequency spectrum  $f(\omega)$ . These quantities are not accessible by the purely static perturbation method and thermodynamic integration technique, respectively. On the other hand, a weak umbrella sampling potential affects the ion's diffusion on the long term, but the characteristics of its short-time behavior should remain visible. Figure 7 compiles  $c_{vv}(t)$  and  $f(\omega)$  for a number of umbrella-windows.

VACF for  $r_0 = 6.3$  Å might be compared to literature results on the binary system water/alkali metal ion (e.g. ref 23). The fairly large K<sup>+</sup> ion differs noticeably from the smaller ("structure making") ions Li<sup>+</sup> and Na<sup>+</sup> and exhibits an exponential decay with strongly damped oscillations (Figure 7a, dashed line). Given the differences in the employed interaction models, the agreement is still acceptable, and it can be assumed that there is no dramatic impact of the umbrella potential on the short-time dynamics ( $\tau < 1.5$  ps).

Experimentally,<sup>24</sup> by infrared spectroscopy ion characteristic frequencies have been detected for Na<sup>+</sup> and K<sup>+</sup>, both in pure solvents and captured in the crown dibenzo-18C6. However, on grounds of transparency in the far IR and solubility, instead of water, the polar solvents dimethyl sulfoxide ( $\mu = 3.9$  D) and pyridine ( $\mu = 2.23$  D) have been used. One strongly cation dependent frequency was identified with the difference in frequency between Na<sup>+</sup> and K<sup>+</sup>, being attributable to their different masses. For K<sup>+</sup> in solution, without crown ether present, this frequency is solvent dependent, but shifts to a solvent independent value of  $167 \pm 3$  cm<sup>-1</sup> in its dibenzo-18C6 complex.

During the simulated association, the maximum in  $f(\omega)$  shifts from  $\omega = 10$  THz = 53 cm<sup>-1</sup> to  $\omega = 28$  THz = 148 cm<sup>-1</sup>, and therefore attains the order of the value measured in ref 24 for the complexed cation. We consider this as evidence for a realistic simulation of the 18C6··K<sup>+</sup> contact pair. A direct experimental access to the vibrational frequency of the complexed K<sup>+</sup> ion in aqueous solution is likely to be impossible due to superimposed modes of water molecules.

Since in the present simulation we have worked without counterion and therefore have neglected the influence of cation-anion interactions, it is also interesting that the frequencies—in the pure solvent as well as in the complex—proved to be independent of the counterion (SCN<sup>-</sup>, BPh<sub>4</sub><sup>-</sup>, PF<sub>6</sub><sup>-</sup>). In ref 24

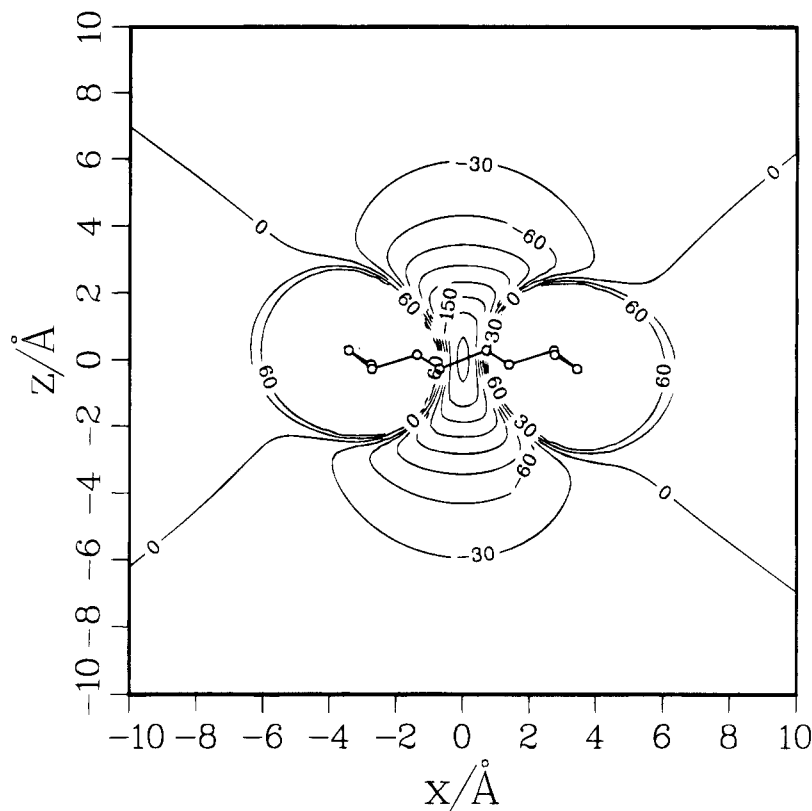


**Figure 6.** Isoenergy contour diagram (kJ/mol) for  $K^+$  in the field of the crown ether molecule (fixed, energy-minimized  $D_{3d}$  conformation, as described in part 1).

it is concluded that in diluted solutions of polar solvents, at least for large and singly charged anions, cation–anion contact pairs can be considered marginally important.

#### 4. Comparison with Previous Works

Finally, the obtained free energy profile is to be compared with two former results, gained by thermodynamic integration<sup>9</sup> and the perturbation method<sup>10</sup> and by using different potential functions and simulation parameters. Except for the fact that the ion is displaced from the crown's center in all three cases, there are profound differences between all results (Figure 8). Particularly, an activation barrier is lacking in the previous results. Instead, only a plateau part is perceivable. When attempting to account for the discrepancies, one must realize first of all that the determination of free energy profiles is rather delicate. It is well-known that thermodynamic integration suffers severely from relaxation errors; perturbation methods need unperturbed configurations which are "sufficiently representative" for the perturbed system; umbrella sampling computations need an adequate sampling of the configuration space (we address our solution of this problem in section 2.3). Moreover, a subtle stability difference between the separated and hydrated solutes on one side and the hydrated solutes in direct interaction on the other side enters the free energy profile.<sup>12</sup> This difference certainly depends sensitively on the employed potential function. Consequently, we go beyond the standard GROMOS potential parameter set and introduce improved interaction potentials, as pointed out in section 2.3.

Two points may be put forth that further support the presence of an activation barrier. To start with, such a barrier is qualitatively in accord with experimental results on the system  $18C6/K^+/H_2O$ .<sup>13</sup> As already noted in ref 9, in the ultrasonic absorption study of ref 13 a barrier has been derived from the temperature dependence of the complexation and decomplex-

ation rates ( $\Delta G_{\text{Kcomplex}}^\ddagger = 26.7$  kJ/mol and  $\Delta G_{\text{Dekomplex}}^\ddagger = 38.8$  kJ/mol) that is—irrespective of all experimental uncertainties—even twice as large as found in our study. On the other hand a barrier in  $W(r)$  has been calculated for a wide variety of other solute pairs (e.g.  $Na^+/Cl^-$ ,<sup>2</sup>  $Ar/Ar$ ,<sup>1</sup> and even benzene/benzene<sup>4</sup>). Very recently, for the solute pair nonactin/ $K^+$  in methanol  $W(r)$  has been reported.<sup>25</sup> The naturally occurring nonactin is an oxygen heterocycle as well. Compared with 18C6, nonactin is nearly twice as large and conformationally more flexible. It contains eight ether oxygens and four exterior carbonyl oxygens. Analogously to our findings, a free energy minimum, corresponding to an arrangement with two bridging methanol molecules, was found at  $r = 4.0$  Å (Figure 8), although this state also involves two carbonyl oxygens interacting with the ion. The deeper minimum in  $W(r)$  can be easily attributed to the weaker solvating and shielding ability of methanol.

In a closer comparison with the literature results it has to be noted that in the (more preliminary) study of van Eerden et al.<sup>9</sup> a too small system has been set up, so that the primary box cannot hold all interacting particles for crown–ion distances up to 7 Å. Moreover, the total simulation time amounts to merely 280 ps, which may not be sufficient to avoid relaxation effects. Beyond that there is a certain analogy to the pair  $Cl^-/Cl^-$  in water. Whereas by thermodynamic integration only a slightly modified repulsion showed up,<sup>12</sup> umbrella sampling revealed a stable, water-bridged state.<sup>3</sup> By now there is increasing experimental evidence for the existence of such  $Cl^- \cdots H_2O \cdots Cl^-$  pairs.<sup>26</sup>

In the perturbation study of Dang and Kollman<sup>10</sup> all six ether oxygens switched to the side of the crown toward the ion, and this conformation (of  $C_2$  symmetry) remained unchanged even for the largest separations between crown and ion. In our simulations the crown ether molecule retains its  $D_{3d}$  geometry (chosen as starting conformation) with only small deviations

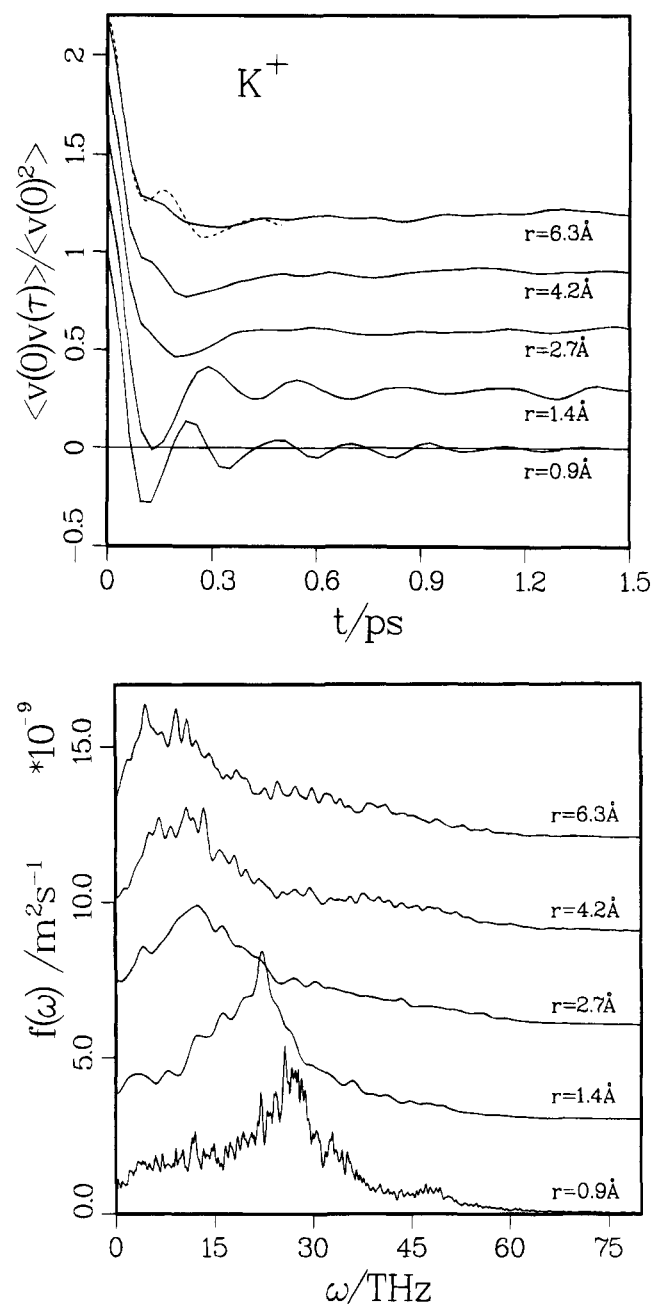


**Figure 7.** VACF (dashed curve from Impey et al.<sup>23</sup> for  $\text{K}^+$  in pure water) and corresponding spectral density  $f(\omega)$  of  $\text{K}^+$  for various umbrella-windows.

(see part 1). Undoubtedly, the particular conformation of the crown has a considerable impact on  $W(r)$ . Of course, for each distance  $r$ ,  $W(r)$  should result from a Boltzmann factor weighted averaging over the crown's total conformation space. Perhaps the  $\text{C}_2$  conformation found in ref 10 is less convenient for a bridging water molecule and therefore allows a more synchronous bond-breaking between the crown and its hydration shell and bond-making between the crown and the ion, without a marked transition state.

Comparison of the computed  $W(r)$  with experimental equilibrium constants is limited due to the fact that the cation has been confined mainly along the crown's symmetry axis during its approach and that  $W(r)$  averaged over the total orientation space remains unknown. As Figure 9 shows, the simulation run for  $r_0 = 3.0$  Å yields a hint that a more lateral attack of the cation is preferred. Whereas in the rest of the umbrella-windows the distribution function for the angle  $\theta = \angle(\vec{n}, \vec{k})$  between the crown's symmetry axis  $\vec{n}$  and the ion's distance vector  $\vec{k}$  revealed

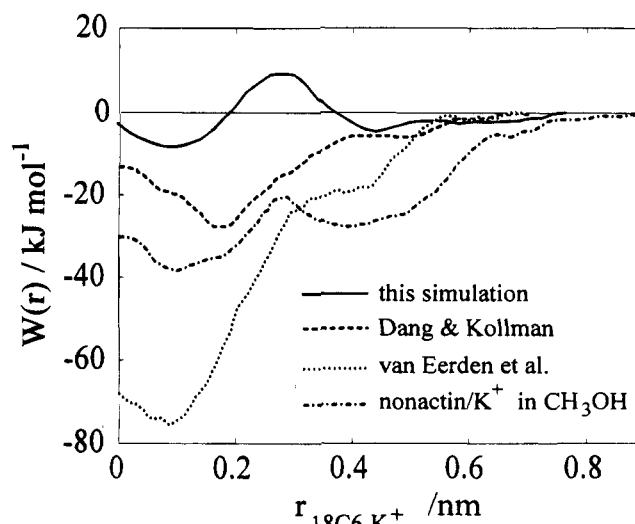


**Figure 8.** Free energy profile  $W(r)$  for  $18\text{C}6 \cdots \text{K}^+$  in water, in comparison with results from refs 9 and 10. Additionally,  $W(r)$  for nonactin/ $\text{K}^+$  in methanol, reported in ref 25, has been inserted.

a maximum at  $\cos \theta = 1$  in correspondence to the applied bias potential, in this case the ion deviates markedly from the symmetry axis's direction. This behavior indicates that by a noncentral approach of the ion and by better interaction with the third ether oxygen not coordinated by the bridging water molecule the complexation step is facilitated. That presumably also explains why during simulation B of the  $18\text{C}6/\text{K}^+$  complex in water (referring to section 4.1 of part 1) a transformation from a contact pair to a solvent-separated pair occurred already after 46 and 180 ps, respectively, despite the considerable barrier in  $W(r)$  for the central approach. As a consequence of this apparently strong angular dependence of the free energy hypersurface, we are not able to present the free energy of complexation  $\Delta G_b$ . Its calculation would require an unjustifiable extrapolation and integration of  $W(r, \theta)$  over the angular space. On the other hand, an exact determination of the full  $W(r, \theta)$  will mean a multiplication of computer time.

## 5. Conclusions and Discussion

In our study, the reaction path in the course of umbrella sampling has been mainly confined to the crown's symmetry axis. The free energy profile mapped in this way provides direct insight into the water influence on the interaction of  $18\text{C}6$  and  $\text{K}^+$  and reveals a solvent-bridged pair  $18\text{C}6 \cdots \text{H}_2\text{O} \cdots \text{K}^+$  as an independent minimum of the free energy profile. A bridging water molecule, already preformed in the binary system  $\text{D}_{3d} - 18\text{C}6/\text{water}$ , proves to be remarkably effective in docking with the  $\text{K}^+$  ion and in blocking the host-guest association. The existence of a barrier for the crossing of the center of the crown—in contrast to the potential energy *in vacuo*—is in accord with former theoretical results by thermodynamic integration<sup>9</sup> as well as the perturbation method.<sup>10</sup> On the other hand the presence of a free energy activation barrier between the contact pair and the solvent-bridged pair conforms qualitatively with experimental results, but is in discordance with refs 9 and 10. The question remains whether the possibility of bypassing the "complexed" water molecule by a more lateral path of the ion, which could reduce the angular averaged free energy barrier at  $r = 2.8$  Å appreciably, is responsible for the lack of this barrier in previous studies. This possibility strongly depends on steric effects, induced by the conformation of the crown ether molecule, but may also be influenced by details of the potential model such as the "united atom" approach of the GROMOS package (see part 1).



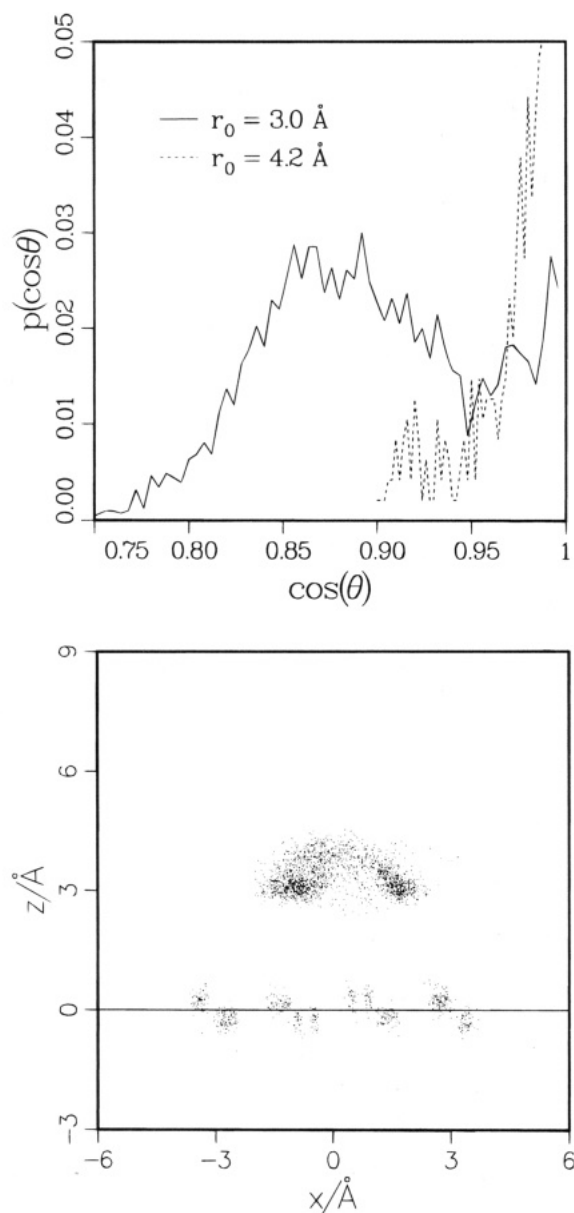


**Figure 9.** (a) Distribution of angle  $\theta$  between the distance vector  $\vec{r}(\text{K}^+/\text{18C6})$  and the crown's symmetry axis for two umbrella-windows. (b) "Dot plot" for umbrella-window  $r_0 = 3.0 \text{ \AA}$  (cf. Figure 2).

There is a special risk that due to limited computing time, inadequately sampled (for molecular solutes ideally over all relative orientations and the whole conformation space) and therefore incomparable  $\Delta G$  values are obtained, without being able to assess quantitatively their accuracy. In this regard umbrella sampling allows for a visual check. By means of the width and smoothness of the distance distribution function within an umbrella-window, one can judge whether for the

present system a convenient bias potential has been employed and whether simulation time has been sufficiently long. In this respect, the present study suggests examining in more detail the full angle dependent free energy surface  $W(r, \theta)$  of the  $\{\text{18C6/K}^+\}_{\text{aq}}$  pair to identify unambiguously the most probable path of approach.

**Acknowledgment.** We thank the "Land Nordrhein-Westfalen" for a scholarship (Th.K.) and the computer center of RWTH Aachen for a generous amount of computing time. Support by the Fonds der Chemischen Industrie is gratefully acknowledged.

#### References and Notes

- (1) Pangali, C.; Rao, M.; Berne, B. J. *J. Chem. Phys.* **1979**, *71*, 2975–2981.
- (2) Berkowitz, M.; Karim, O. A.; McCammon, J. A.; Rossky, P. J. *Chem. Phys. Lett.* **1984**, *105*, 577–580.
- (3) Dang, L. X.; Pettitt, B. M. *J. Phys. Chem.* **1990**, *94*, 4303–4308.
- (4) Ravishanker, G.; Beveridge, D. L. *J. Am. Chem. Soc.* **1985**, *107*, 2565–2566.
- (5) Boudon, S.; Wipff, G. In *Modelling of molecular structures and properties (Studies in physical and theoretical chemistry 71)*; Rivail, J.-L., Ed.; Elsevier: Amsterdam, 1990.
- (6) Zwanzig, R. W. *J. Chem. Phys.* **1954**, *22*, 1420–1426.
- (7) *Computer simulation of biomolecular systems*; van Gunsteren, W. F., Weiner, P. K., Eds.; ESCOM: Leiden, 1989.
- (8) Torrie, G. M.; Valleau, J. P. *J. Comput. Phys.* **1977**, *23*, 187–199.
- (9) van Eerden, J.; Briels, W. J.; Harkema, S.; Feil, D. *Chem. Phys. Lett.* **1989**, *164*, 370–376.
- (10) Dang, L. X.; Kollman, P. A. *J. Am. Chem. Soc.* **1990**, *112*, 5716–5720.
- (11) Guàrdia, E.; Rey, R.; Padró, J. A. *Chem. Phys.* **1991**, *155*, 187–195.
- (12) Guàrdia, E.; Rey, R.; Padró, J. A. *J. Chem. Phys.* **1991**, *95*, 2823–2831.
- (13) Liesegang, G. W.; Farrow, M. M.; Rodriguez, L. J.; Burnham, R. K.; Eyring, E. M. *Int. J. Chem. Kinet.* **1978**, *10*, 471–487.
- (14) Kowall, Th.; Geiger, A. *J. Phys. Chem.* **1994**, *98*, 6216–6224.
- (15) McQuarrie, D. A. *Statistical mechanics*; Harper & Row: New York, 1976. Friedman, H. L. *A course in statistical mechanics*; Prentice-Hall: Englewood Cliffs, NJ, 1985.
- (16) Izatt, R. M.; Bradshaw, J. S.; Nielsen, S. A.; Lamb, J. D.; Christensen, J. J. *Chem. Rev.* **1985**, *85*, 271–339.
- (17) Shchori, E.; Jagur-Grodzinsky, J.; Luz, Z.; Shporer, M. *J. Am. Chem. Soc.* **1971**, *93*, 7133. Shchori, E.; Jagur-Grodzinsky, J.; Shporer, M. *J. Am. Chem. Soc.* **1973**, *95*, 3842–3846.
- (18) Pettitt, B. M.; Karplus, M. *J. Chem. Phys.* **1985**, *83*, 781–789.
- (19) Jorgensen, W. L. *J. Am. Chem. Soc.* **1989**, *111*, 3770–3771.
- (20) Jorgensen, W. L.; Buckner, J. K.; Huston, S. E.; Rossky, P. J. *J. Am. Chem. Soc.* **1987**, *109*, 1891–1899.
- (21) Boudon, S.; Wipff, G.; Maigret, B. *J. Phys. Chem.* **1990**, *94*, 6056–6061.
- (22) Dang, L. X.; Kollman, P. A. *J. Am. Chem. Soc.* **1990**, *112*, 503–507.
- (23) Impey, R. W.; Madden, P. A.; McDonald, I. R. *J. Phys. Chem.* **1983**, *87*, 5071–5083.
- (24) Tsatsas, A. T.; Stearns, R. W.; Risen, W. M., Jr. *J. Am. Chem. Soc.* **1972**, *94*, 5247–5253.
- (25) Marrone, T. J.; Merz, K. M., Jr. *J. Am. Chem. Soc.* **1992**, *114*, 7542–7549.
- (26) Gao, J.; Boudon, S.; Wipff, G. *J. Am. Chem. Soc.* **1991**, *113*, 9610–9614.

JP940747+